Dynamic Modeling and Performance Analysis of Electric Vehicles under Variable Driving Scenarios

Mina BEN RAOUANE [1,*], *Lahcen* BALLI[1], *Isamel* DRIOUCH[1], and *Mohamed* EL HAIM[2]

[1]Engineering Sciences and Applications Laboratory (LSIA), National School of Applied Sciences of Al Hoceima (ENSAH), Abdelmalek Essaadi University, Tetouan, Morocco.
[2]Engineering Sciences and Applications Laboratory (LSIA), Higher School of Technology of Nador (EST Nador), Mohammed First University, Oujda, Morocco.

Abstract. This study presents a dynamic modeling and performance analysis of three electric vehicles (Renault ZOE, Volkswagen ID.3, and Peugeot e-208) developed and simulated using MATLAB/Simulink. Three driving scenarios are investigated: constant-speed operation on flat and inclined roads, tracking of the FTP-75 driving cycle, and a multi-segment trajectory involving successive road slope and direction variations. The resulting analysis provides a rigorous comparative assessment of vehicle speed-tracking accuracy, dynamic behavior, and energy consumption, offering valuable insights into the influence of driving conditions on overall vehicle performance and energy efficiency.
Key Words: *Electric Vehicle, Vehicle Dynamics, Constant Speed Tracking, Driving cycles, MATLAB Simulink.*

1 Introduction

Electric vehicles (EVs) have become a key solution for sustainable mobility, aiming to reduce greenhouse gas emissions and improve overall energy efficiency. Modern EV architectures cover a wide range of powertrain configurations, typically featuring one to four electric motors depending on the vehicle class and design goals [1,2]. Precise modeling of EV dynamics is essential for evaluating energy consumption, optimizing powertrain performance, and developing advanced control strategies across diverse driving conditions. MATLAB/Simulink has emerged as a widely used platform for EV modeling, due to its ability to integrate vehicle dynamics, motor characteristics, and battery behavior within a unified simulation framework [3].

Kirange et al. presented a comprehensive review of dynamic EV performance modeling, highlighting the influence of resistance forces on energy consumption within the Simulink environment. MATLAB/Simulink enables detailed investigations of drivetrain efficiency, energy flow, and vehicle behavior during both traction and regenerative braking modes, while also supporting the implementation of motor control strategies, such as PI controllers, to regulate motor torque and speed effectively [4].

* Corresponding author: mina.benraouane@etu.uae.ac.ma

Recent studies, such as those by Almadani et al., further demonstrate the scalability and versatility of MATLAB/Simulink-based approaches by extending dynamic performance analysis to three-wheelers under multiple standard driving cycles, such as FTP-75, and testing protocols like WLTP. These modeling and simulation capabilities provide valuable insights for designing efficient and reliable EV systems under real-world operating conditions [5].

Similarly, Yin et al. proposed a forward simulation-based integrated EV model to overcome the high cost and long testing cycles associated with conventional real-vehicle evaluation methods. Based on longitudinal dynamics theory and specific EV parameters, a high-fidelity MATLAB/Simulink model was developed and validated using actual driving cycles as input conditions [6].

This study develops a detailed dynamic model of an electric vehicle and conducts a comparative performance assessment of three production EVs (Renault ZOE, Volkswagen ID.3, and Peugeot e-208) using MATLAB/Simulink. In addition, a comprehensive Table 1 is included to summarize the key technical characteristics of the selected vehicles, providing a clear basis for model parameterization and comparative analysis.

Table 1. Technical parameters of the electric vehicles used in the simulation study.

Parameter	Renault ZOE	VW ID.3	Peugeot e-208	Unit
Vehicle mass (Mv)	1502	1985	1455	kg
Wheel radius (Rw)	0.305	0.351	0.300	m
Gear ratio	9.34	10.0	9.0	–
Transmission efficiency	0.95	0.99	0.97	–
Motor efficiency	0.92	0.97	0.93	–
Battery efficiency	0.97	0.95	0.95	–
Drag coefficient (Cx)	0.29	0.274	0.33	–
Frontal area (S)	2.59	2.37	2.25	m^2
Rolling resistance coefficient (Crr)	0.010	0.0105	0.011	–
Air density (ρ)	1.225	1.225	1.225	kg/m^3
Gravity (g)	9.81	9.81	9.81	m/s^2

2 Methodology

This study investigates the dynamic and energetic behavior of three electric vehicles (Renault ZOE, Volkswagen ID.3, and Peugeot e-208). To this end, three driving scenarios were defined, each designed to evaluate a specific aspect of vehicle performance:

Scenario 1: Constant-Speed Tracking on Flat and Inclined Road Profiles.

The first scenario evaluates the ability of each vehicle to maintain a prescribed constant speed under two distinct road conditions:

- Flat road
- Inclined road characterized by a slope angle of 0.2 rad

The objective is to analyze the impact of road grade on motor torque, motor rotational speed, and battery power, in order to assess the additional traction effort and energy demand required to compensate for the increased load induced by the road incline.

Scenario 2: Tracking of the FTP-75 Driving Cycle on Flat and Inclined Roads.

The second scenario employs the standard FTP-75 driving cycle as the reference speed input. The vehicle responses are evaluated under two configurations:

- Flat road,
- Inclined road with a slope angle of 0.2 rad

This scenario allows the characterization of vehicle dynamic behavior under a representative urban driving cycle, both with and without the influence of road elevation.

Scenario 3: Response to Successive Slope Variations (Multisegment Trajectory).

The third scenario evaluates the vehicle dynamic behavior along a multisegment trajectory with successive changes in road slope. The trajectory comprises ten consecutive phases:

- **Step 1:** Straight-line motion at 40 km/h;
- **Step 2:** Right turn at 20 km/h;
- **Step 3:** Straight segment at 20 km/h;
- **Step 4:** Left turn at 20 km/h;
- **Step 5:** Additional straight segment at 20 km/h;
- **Step 6:** Ascending segment at 0.2 rad with linear acceleration to 100 km/h;
- **Step 7:** Flat-road segment at a constant speed of 100 km/h;
- **Step 8:** Descending segment with a negative slope of −0.2 rad;
- **Step 9:** Linear deceleration from 100 km/h to 20 km/h;
- **Step 10:** Final linear deceleration to 10 km/h.

This multisegment trajectory provides a rigorous framework for analyzing vehicle stability, powertrain performance, and energy consumption under dynamically varying operating conditions.

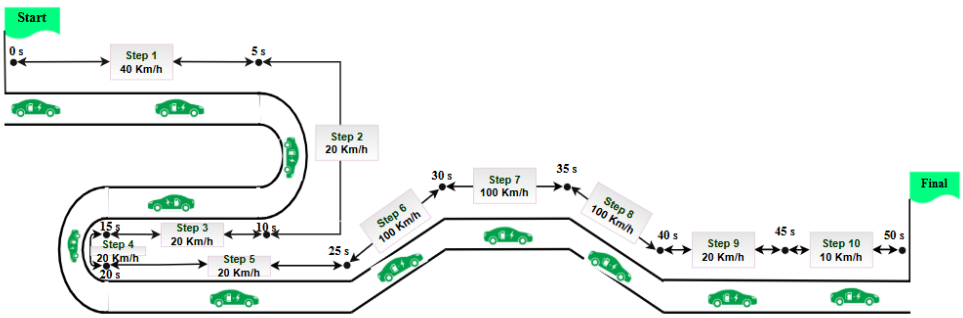

Fig. 1. Reference Driving Cycle Profile for the Electric Vehicle Study.

3 Electric Vehicle Modeling

3.1 Vehicle Dynamics

3.1.1 Aerodynamic Force

The aerodynamic drag force Faero, is the resistive force generated by the relative motion between the vehicle and the surrounding air. It originates from pressure differentials and

viscous effects acting on the vehicle body. This force depends on the air density ρ (kg/m^3), the vehicle frontal area S (m^2), and the aerodynamic drag coefficient Cx, and it increases proportionally to the square of the vehicle's longitudinal speed V_{veh} (m/s) [3,7]:

$$F_{aero} = \frac{1}{2}\rho\, C_x\, A\, {V_{veh}}^2 \quad (1)$$

3.1.2 Rolling Resistance Force

The rolling resistance force, which arises from the interaction between the tires and the road surface, is expressed as [7]:

$$\mathrm{F_{roll}} = \mathrm{g\, M_v\, C_{rr} \cos(\boldsymbol{\alpha})} \quad (2)$$

Where:

Mv: Vehicle mass[kg].
g: Gravitational acceleration [m/s^2].
Crr: Rolling resistance coefficient
α: Road slope angle [rad].

3.1.3 Gravitational Force

During uphill and downhill driving conditions, the longitudinal component of the gravitational force acting along the road slope is expressed as follows [3,7]:

$$\mathrm{F_g} = \mathrm{g\, M_v \sin(\boldsymbol{\alpha})} \quad (3)$$

3.1.4 Acceleration Force

The acceleration force is given by [7,8]:

$$\mathrm{F_{acc}} = \mathrm{M_v} \frac{\mathrm{dV_{veh}}}{\mathrm{dt}} \quad (4)$$

3.1.5 Total Force

The total longitudinal force applied to the vehicle is expressed as the combination of the resistive forces opposing motion and the inertial force resulting from longitudinal acceleration [3,7,8]:

$$\mathrm{F_{tot}} = \mathrm{F_{aero}} + \mathrm{F_{roll}} + \mathrm{F_g} + \mathrm{F_{acc}} \quad (5)$$

3.1.6 Wheel Rotational Speed

The wheel rotational speed, expressed in revolutions per minute (rpm), is derived from the vehicle's linear velocity according to the following relationship [7]:

$$\Omega_{\mathrm{wheel}} = \frac{60 \times \mathrm{V_{veh}}}{2\pi \times \mathrm{R_w}} \quad (6)$$

Ω_{wheel} is the wheel rotational speed (rpm), R_w is the wheel radius (m), V_{eh} is the vehicle speed in m/s.

3.1.7 Wheel Torque

The torque at the wheel is expressed as [8]:

$$T_{wheel} = F_{tot}\, R_w \quad (7)$$

3.2 Transmission Modeling

The vehicle employs a single-speed reduction gear, and the kinematic relationships linking the motor variables to the wheel variables are expressed as [9]:

$$\Omega_{motor} = G \times \Omega_{wheel} \quad (8)$$

$$T_{wheel} = G \times \eta_{tans} \times T_{motor} \quad (9)$$

Where:

Ωmotor is the motor rotational speed (rpm), G is the reduction ratio and η_{trans} is the transmission efficiency.

3.3 Electric Motor Modeling

The motor output power is evaluated from the product of torque and rotational speed, with the efficiency of the motor explicitly considered [10]:

$$P_{motor} = \frac{2\pi \times \Omega_{motor} \times T_{motor}}{60 \times \eta_{motor}} \quad (10)$$

Where:

P_{motor} is the electrical power [W], Ω motor is speed [rpm], T_{motor} is torque [Nm], and η_{motor} is the motor efficiency.

3.4 Battery Energy Modeling

The battery model relies on a power balance formulation, according to which the electrical power extracted from the battery is given by [9,11]:

$$P_{bat} = \begin{cases} \frac{P_{motor}}{\eta_{bat}} & \text{if } P_{motor} > 0 \\ 0 & \text{if } P_{motor} < 0 \end{cases} \quad (11)$$

The energy consumed by the battery is then evaluated according to [9,12]:

$$E_{bat}(kWh) = \frac{P_{bat}(W) \times t(h)}{1000} \quad (12)$$

Where:

P_{bat} is the battery electrical power [W], η_{bat} is the battery efficiency, E_{bat} is the battery energy consumption [kWh], and t is the operating time [h].

4 Results and Discussion

In this study, comprehensive dynamic models of three electric vehicles are developed and simulated using MATLAB/Simulink. The models incorporate the vehicle longitudinal dynamics, electric motor and transmission characteristics, and the battery power flow.

4.1 Scenario 1: Constant-Speed Tracking on Flat and Inclined Road Profiles.

The objective of this scenario is to evaluate the dynamic response and energy consumption of three electric vehicles (Renault ZOE, Volkswagen ID.3, and Peugeot e-208) operating at a constant cruising speed of 100 km/h (Fig. 2) under two distinct road conditions.

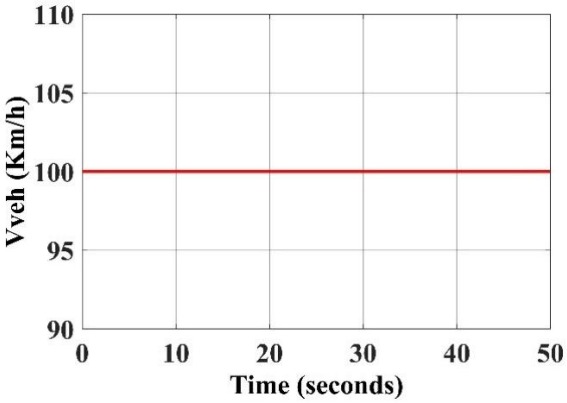

Fig. 2. Constant driving speed.

4.1.1 Flat road

Fig. 3 illustrates the evolution of the traction motor torque for the three electric vehicles during the constant-speed tracking scenario. The results highlight a clear disparity in torque demand among the vehicles. The Volkswagen ID.3 exhibits the highest required torque (≈18.13 N·m), followed by the Peugeot e-208 (≈17.45 N·m), whereas the Renault ZOE shows the lowest torque demand (≈17.26 N·m).

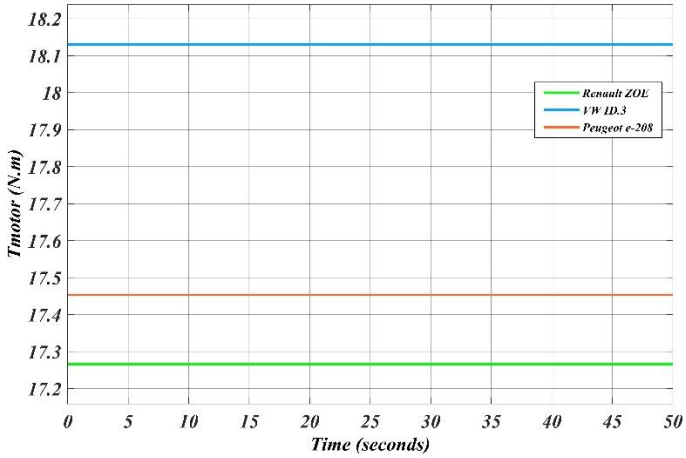

Fig. 3. Motor torque profiles of three EV models at constant driving speed (Flat Road).

Fig. 4 presents the corresponding motor rotational speeds. The Renault ZOE operates at the highest rotational speed (≈8123 rpm), while the Volkswagen ID.3 records the lowest value (≈7557 rpm).

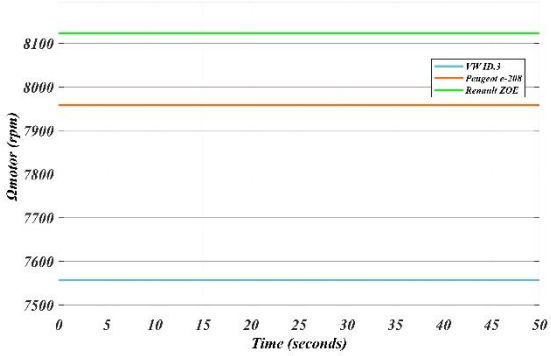

Fig. 4. Motor rotational speed profiles of three EV models at constant driving speed (Flat Road).

Fig. 5 depicts the electrical power drawn from the battery under constant-speed conditions. The Peugeot e-208 shows the highest power demand (≈16.46 kW), whereas the Volkswagen ID.3 demonstrates the lowest consumption (≈15.57 kW), indicating superior energy efficiency. The Renault ZOE presents an intermediate power level (≈16.45 kW).

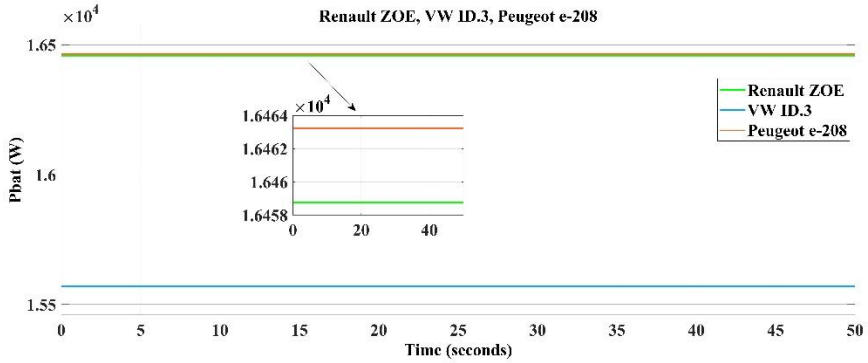

Fig. 5. Battery power profiles of three EV models at constant driving speed (Flat Road).

4.1.2 Inclined road (0.2)

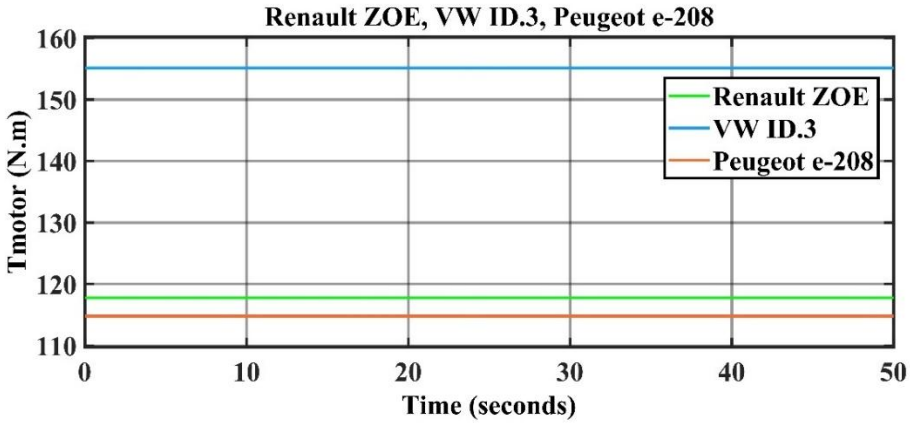

Fig. 6. Motor torque profiles of three EV models at constant driving speed (0.2 rad).

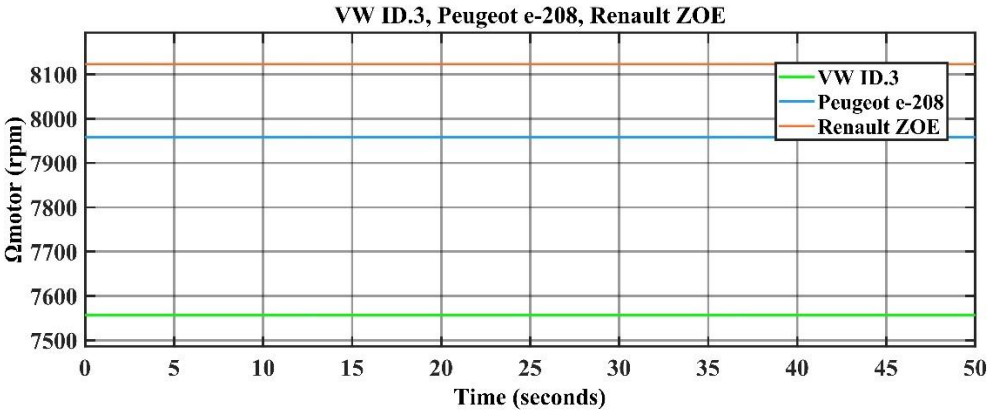

Fig. 7. Motor rotational speed profiles of three EV models at constant driving speed (0.2 rad).

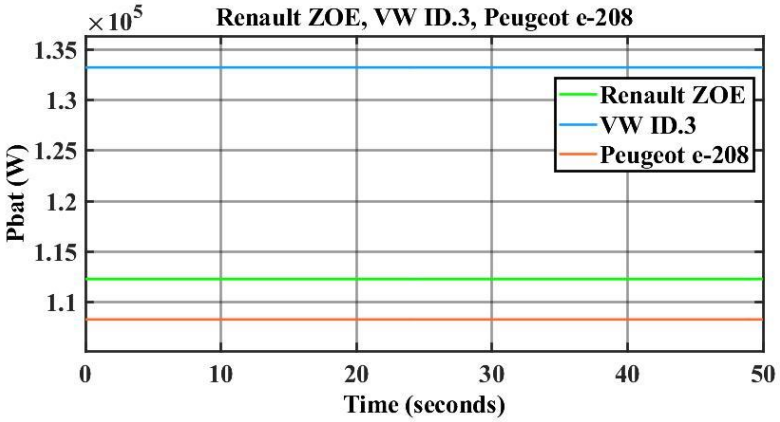

Fig. 8. Battery power profiles of three EV models at constant driving speed (0.2 rad).

When operating on an inclined road, all three electric vehicles experience a marked increase in motor torque relative to the flat-road condition (Fig. 6). This increase results from the additional longitudinal gravitational force component, which is proportional to the vehicle mass and the sine of the road inclination angle, sin(α). The Volkswagen ID.3 exhibits the highest torque requirement (≈155 N·m), followed by the Renault ZOE (≈117 N·m), while the Peugeot e-208 presents the lowest torque demand (≈115 N·m).

Motor rotational speeds remain nearly unchanged across all vehicles (Fig. 7), as they are primarily determined by the imposed vehicle speed and the fixed transmission ratio. Consequently, the road gradient predominantly affects the torque demand rather than the motor speed.

As illustrated in Fig. 8, the battery electrical power demand increases significantly for all vehicles under uphill conditions due to the higher mechanical effort required to overcome gravitational resistance. The Volkswagen ID.3 records the highest power consumption (≈133.24 kW), whereas the Peugeot e-208 shows the lowest demand (≈108.27 kW). The Renault ZOE again exhibits intermediate behavior, with a power requirement of approximately 112.27 kW.

4.2 Scenario 2: Tracking of the FTP-75 Driving Cycle on Flat and Inclined Roads.

The second scenario assesses the capability of the three electric vehicles under investigation (Renault ZOE, Volkswagen ID.3, and Peugeot e-208) to accurately follow the standardized FTP-75 driving cycle. This cycle is representative of urban driving conditions, characterized by frequent stop-and-go phases, rapid accelerations, and repeated decelerations. Figure 9 presents the FTP-75 speed profile adopted as the reference input for the simulations, which were conducted under two distinct road configurations.

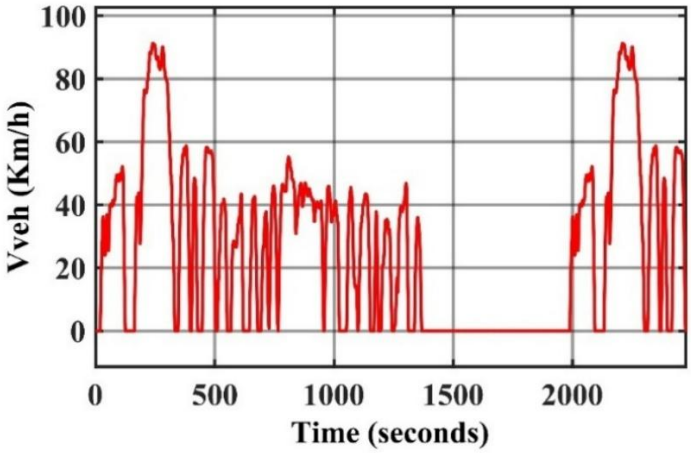

Fig. 9. Speed Profile of the FTP-75 Driving Cycle.

4.2.1 Flat road

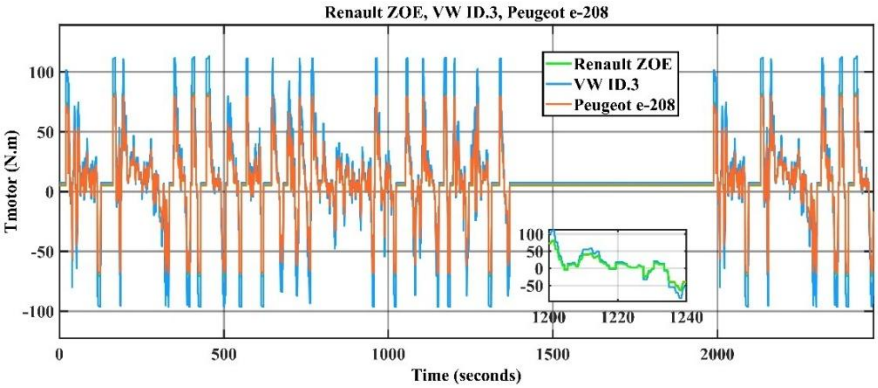

Fig. 10. Motor torque profiles of three EV models during the FTP-75 driving cycle (Flat Road).

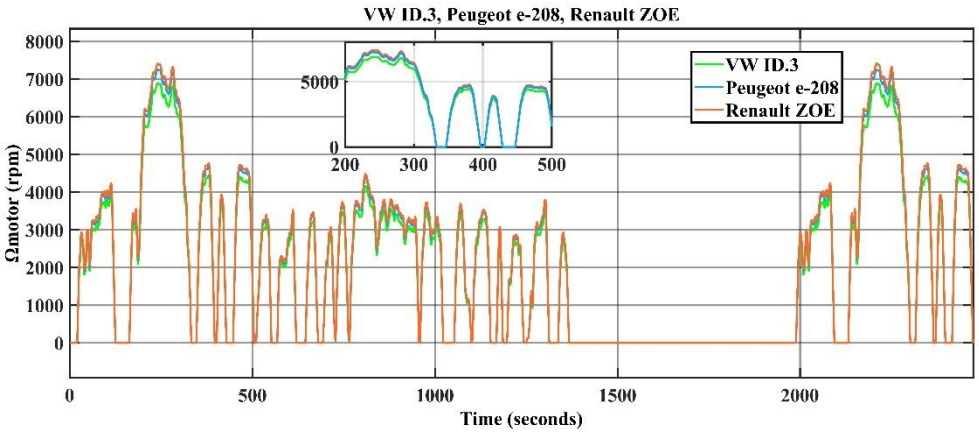

Fig. 11 Motor rotational speed profiles of three EV models during the FTP-75 driving cycle (Flat Road).

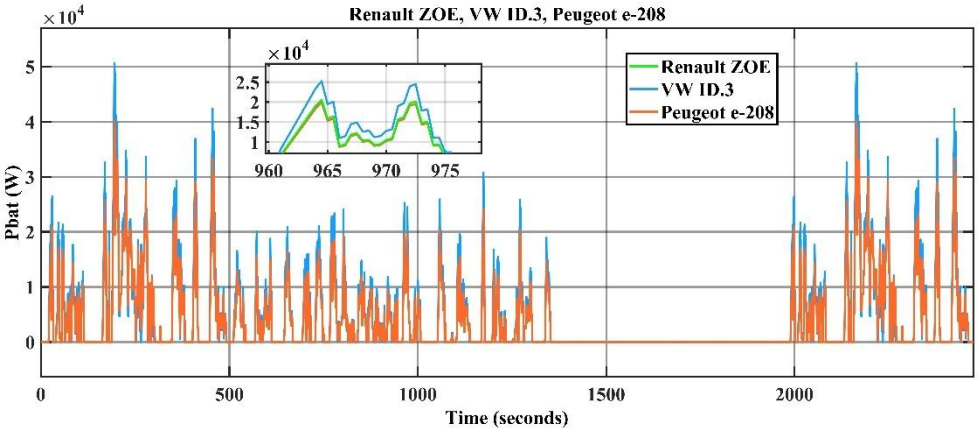

Fig. 12. Battery power profiles of three EV models during the FTP-75 driving cycle (Flat Road).

Figure 10 illustrates the temporal evolution of the motor torque during the FTP-75 driving cycle. The results reveal rapid and recurrent torque fluctuations associated with successive acceleration and deceleration phases inherent to the cycle. All three vehicles display a comparable oscillatory trend; however, the Volkswagen ID.3 exhibits the highest torque amplitude (≈112 N·m), which can be attributed to its higher rated motor power. Positive torque values correspond to traction phases, whereas negative torque values indicate regenerative braking events.

Figure 11 presents the motor rotational speed profiles, which closely follow the reference vehicle speed trajectory. For all vehicles, sharp increases in rotational speed are observed during acceleration phases, followed by abrupt reductions during deceleration periods characteristic of the FTP-75 cycle. Among the three models, the Renault ZOE reaches slightly higher peak motor speeds (≈7412 rpm) compared to the Volkswagen ID.3 and the Peugeot e-208.

Figure 12 depicts the battery electrical power demand throughout the FTP-75 cycle, highlighting pronounced power fluctuations driven by the highly transient nature of urban driving conditions. The highest power peaks are observed during rapid acceleration events, particularly for the Volkswagen ID.3 (≈50.6 kW). These results indicate that the FTP-75

cycle imposes significant dynamic loading on the battery–motor system, underscoring the strong influence of urban driving patterns on energy consumption and on the sizing requirements of electric powertrain components.

4.2.2 Inclined road (0.2)

Figure 13 shows that, under positive road slope conditions, the motor torque profiles exhibit significantly higher amplitudes compared with the flat-road case, owing to the additional gravitational load acting along the direction of motion. Among the three vehicles, the Volkswagen ID.3 presents the highest torque demand (≈250 N·m), whereas the Renault ZOE (≈184 N·m) and the Peugeot e-208 (≈178.7 N·m) display lower and closely comparable torque levels.

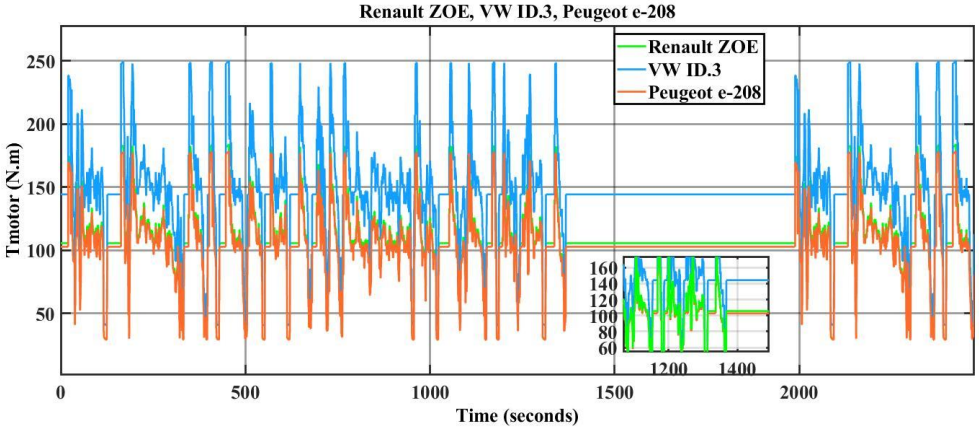

Fig. 13. Motor torque profiles of three EV models during the FTP-75 driving cycle (0.2).

As illustrated in Figure 14, the motor rotational speed closely follows the FTP-75 reference speed profile, with slightly increased peak values under inclined-road conditions. The Renault ZOE reaches the highest rotational speed (≈7412 rpm), while the Volkswagen ID.3 and the Peugeot e-208 exhibit similar but lower maximum speeds.

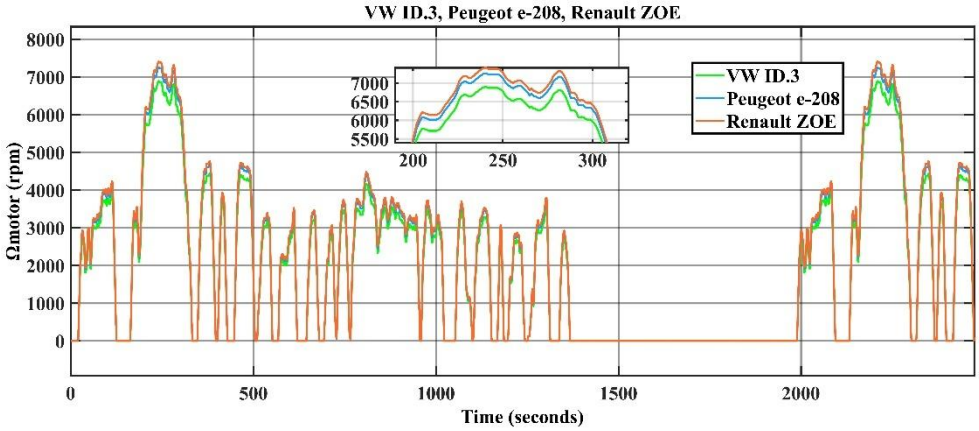

Fig. 14. Motor rotational speed profiles of three EV models during the FTP-75 driving cycle (0.2).

Figure 15 indicates a substantial increase in battery electrical power demand on the inclined road, particularly during acceleration phases. The Volkswagen ID.3 records the highest

power peaks (≈140 kW), confirming the combined effect of road gradient and higher vehicle mass on the overall energy demand.

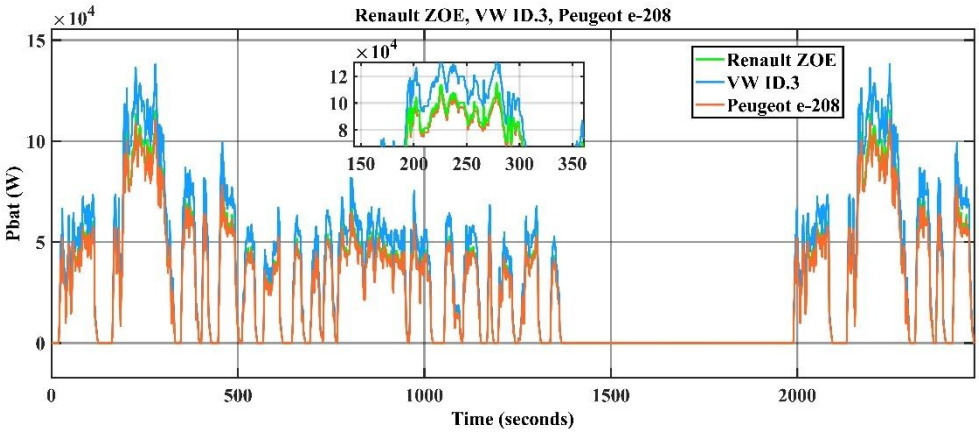

Fig. 15. Battery power profiles of three EV models during the FTP-75 driving cycle (0.2).

4.3 Scenario 3: Response to Successive Slope Variations (Multisegment Trajectory).

This scenario reproduces realistic driving conditions in which the vehicle is subjected to successive uphill and downhill segments while maintaining a constant target speed.
The objective is to assess the influence of road grade variations on motor torque, motor rotational speed, and battery electrical power demand. Figure 16 presents the vehicle speed profile corresponding to a real multi-segment driving trajectory used in the simulations.

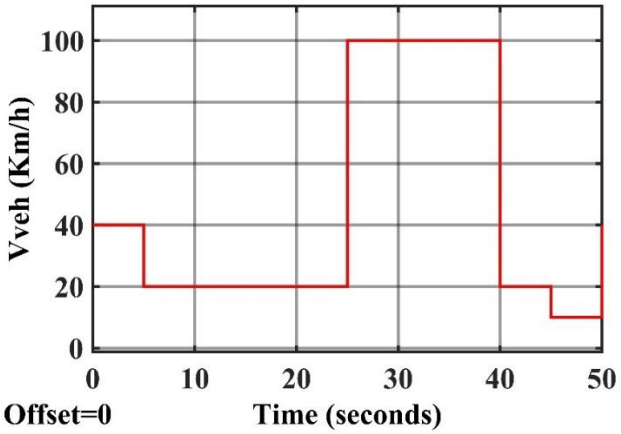

Fig. 16. Speed Profile During Successive Slope Transitions.

As illustrated in Fig. 17, all vehicles exhibit an increase in motor torque during positive road gradients, while negative torque values are observed during downhill segments, corresponding to regenerative braking operation. The highest torque peaks occur during the steepest uphill sections, with the Volkswagen ID.3 requiring the largest torque (≈155 N·m), whereas the Peugeot e-208 shows the lowest demand (≈115 N·m).

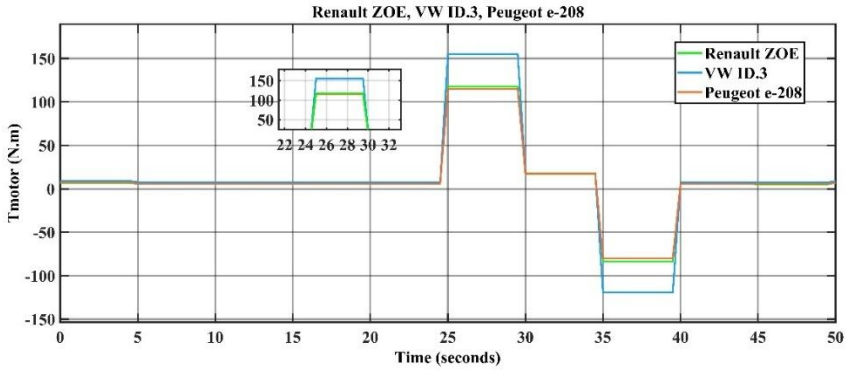

Fig. 17. Motor Torque Response of the Three EV Models to Grade Variations.

Fig. 18 indicates that the motor rotational speed remains nearly constant within each road-grade segment, confirming effective speed regulation despite slope-induced disturbances. Small differences among the three vehicles can be attributed to variations in transmission ratios and drivetrain efficiencies, with the Renault ZOE operating at slightly higher rotational speeds (≈8120 rpm).

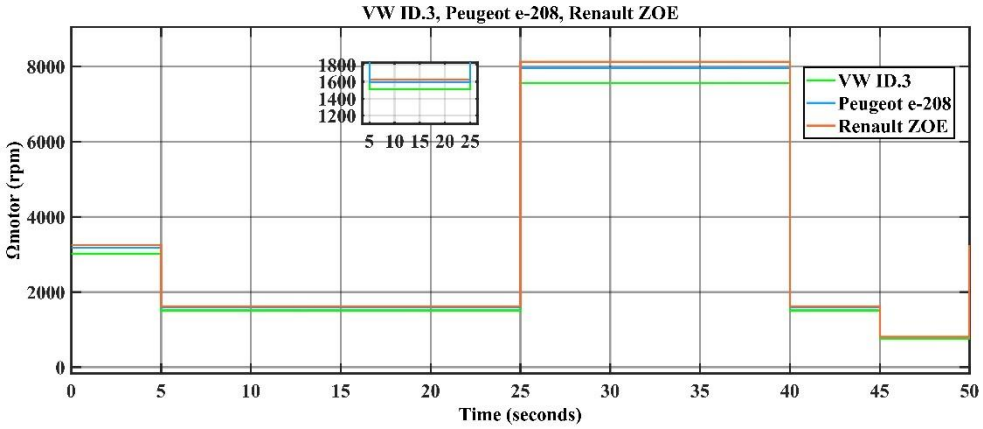

Fig. 18. Motor rotational Speed Evolution Under Variable Road Slope Conditions.

Fig. 19 presents the battery electrical power profile, showing a sharp increase in power demand during uphill segments and negative power values during downhill phases, which reflect regenerative energy recovery. Under identical driving conditions, the Peugeot e-208 exhibits the lowest electrical power demand (≈108.275 kW), whereas the Volkswagen ID.3 requires higher power levels (≈133.241 kW).

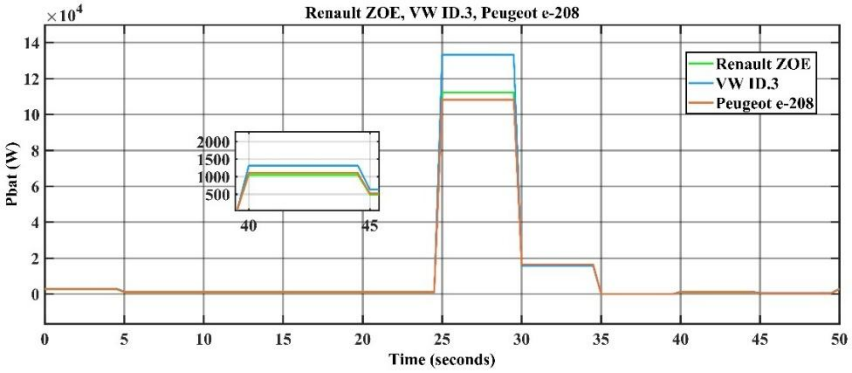

Fig. 19. Battery Power Demand During Successive Slope Transitions.

Conclusion

The comparative analysis demonstrates that vehicle mass and drivetrain characteristics strongly affect motor torque, rotational speed, and energy consumption. Road inclinations lead to substantial increases in torque and battery power demand, whereas motor rotational speed remains primarily determined by vehicle speed and transmission ratio. The FTP-75 driving cycle produces pronounced torque and power fluctuations, emphasizing the impact of urban driving conditions on battery–motor system stress. Overall, efficient energy management and the use of regenerative braking are critical to mitigate the increased electrical and mechanical loads under realistic driving scenarios.

While the present study is limited to simulation-based analysis, experimental validation under real driving conditions constitutes a relevant extension of this work and is intended to be addressed in future research in order to further assess the accuracy and robustness of the proposed modeling framework.

Acknowledgments

I would like to express my sincere gratitude to the CNRST for its support through the "PhD-Associate Scholarship – PASS" program.

References

1. O. Nezamuddin, R. Bagwe, E. dos Santos Jr., A multi-motor architecture for electric vehicles, in 2019 IEEE Transportation Electrification Conference and Expo (ITEC) (2019).
2. S. De Pinto, P. Camocardi, C. Chatzikomis, A. Sorniotti, F. Bottiglione, G. Mantriota, P. Perlo, On the comparison of 2- and 4-wheel-drive electric vehicle layouts with central motors and single- and 2-speed transmission systems. Energies 13, 3328 (2020).
3. M. Al Halabi, A. Al Tarabsheh, Modelling of electric vehicles using Matlab/Simulink, in SAE Technical Paper (2020).
4. Y.K. Kirange, V.S. Patil, K.L. Patil, S.R. Patel, H.S. Sapkale, J.B. Patil, An overview of Matlab/Simulink dynamic model of an electric vehicle's performance. Int. J. Eng. Res. Technol. (2023)

5. M.M.M. Almadani, O.M. Longe, L. Olatomiwa, T. Somefun, Analysis of the dynamic performance and energy efficiency of a three-wheel electric vehicle under standard drive cycles. AIMS Energy (2026)
6. X. Yin, L. Zheng, J. Hu, W. Li, Modeling and Road Condition Simulation Analysis of Electric Vehicle Integrated Model, J. Innov. Dev. (2025).
7. Hitesh S., C. Sunanda, Modeling and performance analysis of an electric vehicle with MATLAB/Simulink. Int. Res. J. Eng. Technol. 7, Issue 6 (2020).
8. A. Nouh, Contribution to the development of a simulator for road electric vehicles, Ph.D. thesis, University of Technology of Belfort-Montbéliard and University of Franche-Comté (2008)
9. L. Simchon, R. Rabinovici, Real-time implementation of green light optimal speed advisory for electric vehicles. Vehicles 2 (2020)
10. P.D. Walker, S. Abdul Rahman, B. Zhu, and N. Zhang, Modelling, Simulations, and Optimisation of Electric Vehicle Powertrains, Adv. Mech. Eng. (2013).
11. R. M. Figueiredo, Aircraft electric propulsion systems: Alternative energy storage and electric motors, Master Thesis, Técnico Lisboa, Novembre (2022).
12. A.Ceschia, Optimal Design Methodology of Embedded Energy Conversion Chains, Ph.D. Thesis in Electrical Energy Engineering, Université Paris-Saclay, France (2020).